Christopher M. Rozoff *, W. D. Terwey, M. T. Montgomery, and W. H. Schubert

Dept. of Atmospheric Science, Colorado State Univ., Fort Collins, Colorado

1. INTRODUCTION

For eye walls, eye wall replacement cycles, and rain-bands, convection is fundamental to the hurricane. As hurricane modeling resolves convective processes in modern research, characterizing the evolution of individual convective storms in tropical cyclones is an important step toward understanding basic intensity change. Because the environments of these structural features contain a breadth of thermodynamic and kinematic states for convection to contend with, there are potentially a variety of convective morphologies that can occur in hurricanes.

One phenomenon associated with rapid intensity fluctuation in hurricanes is the secondary eye wall and the eye wall replacement cycle (Willoughby et al. 1982). Using the basic dynamics of two-dimensional (2D) stirring, Rozoff et al. (2006) hypothesize that in the formation of the moat between the eye walls, horizontal straining flow outside strong hurricane cores rapidly filaments convection.   Thus, in combination with subsidence warming and drying common in the moat, convection becomes unlikely at these radii outside a primary eye wall.   However, proper quantification of these 2D rapid filamentation ideas requires the treatment of three-dimensional (3D) cloud models. As an example of real-world complexity not accounted for in 2D theory, vertical shear has been shown to organize convective clouds into long-lived systems (e.g., Weisman and Rotunno 2004; Klemp 1987); therefore, a combination of horizontal and vertical shears may be expected to induce positive feedbacks on convection unless sufficiently strong shear leads to the detrimental effect is described in Rozoff et al. (2006).

Using a 3D cloud-resolving model, this talk explores the response of convection to systematic variations in hurricane-like vertical and horizontal shears and thermodynamics profiles. Expanding upon the work of Rozoff et al. (2006), an understanding of convective organization to various shears and a practical threshold for adverse shear are sought.   Additionally, this research addresses the basic changes convection may impart on the lifetimes and morphology of future convection by interaction with the mean flow (e.g., Möller and Montgomery 2000; Möller and Shapiro 2005), which may inspire new hypotheses in the areas of secondary eye wall formation, spiral band structures, and hurricane rainfall efficiency.
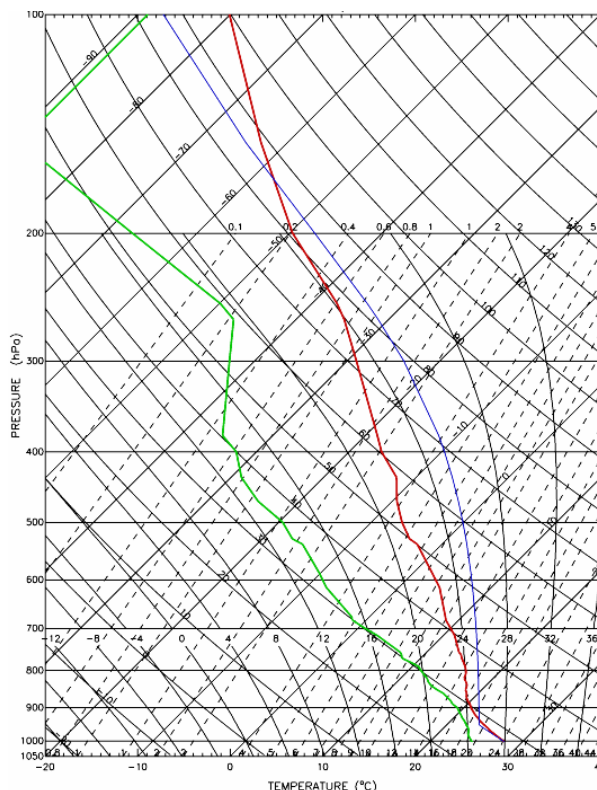
---

* *Corresponding author address*: Christopher M. Rozoff, Colorado State University, Dept. of Atmospheric Science, Fort Collins, CO 80523; e-mail: rozoff@atmos.colostate.edu.

Figure 1: Skew-*t* log-*p* profile of dew point (green curve; ^{o}C), temperature (red curve; ^{o}C), and hypothetical, undiluted, surface-based parcel path temperature (blue curve; ^{o}C).

2. METHODOLOGY

The Regional Atmospheric Modeling System (RAMS) version 4.3 (Cotton et al. 2003) is chosen for this idealized study.   RAMS is 3D, nonhydrostatic, and compressible and it has been used extensively in cloud dynamics studies (Cotton et al. 2003).   Grid spacing of 500 m is utilized over one 125 km wide horizontal grid on the *f*-plane.   In the vertical, a stretched Cartesian coordinate is employed over a depth of 25 km, containing grid spacing of 160 m near the surface to a maximum spacing of 500 m. The experiments neglect radiation and assume a free slip lower boundary. Gravity wave reflection is minimized at the top and lateral boundaries.

The initial thermodynamic profile is compiled from a series of dropsondes and a nearby proximity sounding outside the core of Hurricane Isabel (2003) (Figure 1). In this sounding, there is 2067 J kg^{-1} surface-based convective available potential energy (CAPE) and only 1 J kg^{-1} convective inhibition (CIN). It is worth pointing out

the dry and unstable air aloft and the nearly convectively neutral and moist low-levels.

Cumulonimbus convection is initiated with a warm bubble. Sixteen numerical experiments are performed with the convection by systematically varying hurricane-like shear profiles in both the vertical and horizontal. The initial wind profile takes the form

$$v(x, y, z, t) = v_z z + v_x x + v_{ref}, \qquad (1)$$

where v_z is the vertical wind shear, which remains constant up to 15 km and vanishes at higher altitudes, v_x is the constant horizontal wind shear, and v_{ref} is formulated such that storm advection is minimized away from the domain center. The experiments vary v_z over the values of 0, 5, 10, and 20 m s^{-1} per 15 km and v_x takes on the values 0, -2, -4, and -6 x 10^{-4} s^{-1}. All cases are initialized in geostrophic and hydrostatic balance. Given the anticyclonic shear across the domain to emulate the shear outside a hurricane vortex, to ensure inertial stability, the constant Coriolis parameter, f, is adjusted such that the initial absolute vorticity, $v_x + f$, is always equal to 1 x 10^{-4} s^{-1}. This condition approximately holds, along with the neglect of curvature vorticity, for a domain rotating about an axisymmetric vortex at radii just outside the radius of maximum winds to about 100 km. Therefore, as the horizontal shear increases, some typical kinematic environments of rain-bands to tropical cyclone moats are covered.

3. CONVECTIVE RESPONSE TO SHEAR

To understand the effects of shear on a heat source, the early evolution of the warm bubble is examined before discussing the convective morphology. Without environmental shear, the initial heat plume grows upright and axisymmetric about the center of initial heating and the flow completes an axisymmetric overturning circulation. By 0.6 hr, the plume acquires vorticity of 4 x 10^{-4} s^{-1}. A vorticity budget shows this vorticity is spun up by the convergence of the background f at low levels. Upward motion transports this vorticity throughout the plume. When vertical shear is applied to the convective plume, the overturning plume is tilted toward the north with height. The compensating downdraft is strongest downshear of the updraft. The vorticity budget shows, consistent with the results of Klemp (1987) and others, that tilting of environmental horizontal vorticity leads to the formation of a vorticity dipole, where anticyclonic and cyclonic vorticity occur on the western and eastern flanks of the plume. Because of the concurrent convergence of positive f, the cyclonic vorticity is greater than anticyclonic vorticity in the dipole.

Horizontal shear leads to elliptical organization of the heat plume. This organization is well illustrated in the vertical velocity fields at 1.2 km height (near the top of the plume), as shown in Figure 2. Here, the vertical motion pattern is banded, with upward motion in the center of the plume and downward motion on the parallel flanks of the ellipse's major axis. At the plume's top, outward motion is also mostly restricted to the
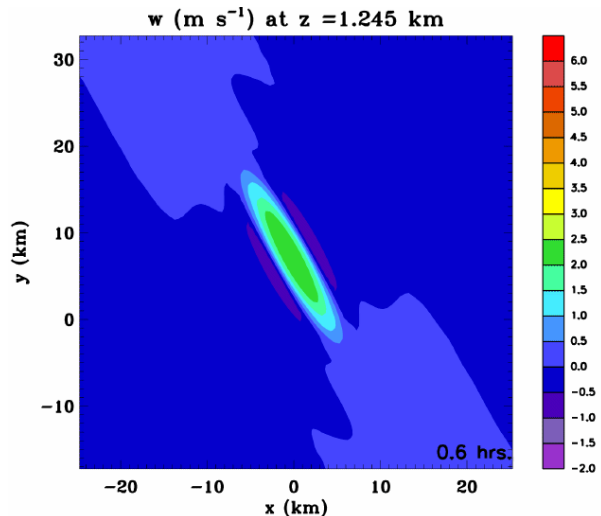

Figure 2: Vertical velocity (m s^{-1}) at z = 1.245 at 0.6 hr for the experiment with v_x = -6 x 10^{-4} s^{-1} and v_z = 0.

parallel flanks. Similarly, low-level inflow is most marked on the same flanks.

Near the top of the plume, an interesting quadrupole pattern of vorticity emerges. Rotating the Cartesian grid surrounding the banded structure in Figure 2 to align with the ellipse's major axis allows for a more illuminating analysis of the vorticity budget. It turns out the only term in the vorticity budget responsible for the quadrupole pattern is the tilting term. The tilting term is defined in the new (x,y)-coordinate system as

$$\left.\frac{\partial \zeta}{\partial t}\right|_{tilt} = \frac{\partial w}{\partial y}\frac{\partial u}{\partial z} - \frac{\partial w}{\partial x}\frac{\partial v}{\partial z}, \qquad (2)$$

where u, v, and w are the x, y, and z components of the wind and ζ is the relative vorticity. Each derivative on the right-hand side of (2), along with the total tilting term, is plotted in Figure 3. Clearly, the tilting term is dominated by the tilting of horizontal vorticity created by the overturning circulation at the ends of the elliptical plume. The strong gradients in w formed in the transverse direction are responsible for tilting the horizontal vorticity. Weaker gradients along the major axis restrict comparable tilting of horizontal vorticity on the parallel flanks. Thus, horizontal shear plays an important role in forming banded structures with heat plumes.

When both vertical and horizontal shear coexist, the plume properties reflect a combination of those seen in the previously described results. Although horizontal shear stretches the plume into an ellipse with a banded overturning structure, more outward flow occurs on the up-shear side of the ellipse. A vorticity budget shows the asymmetric quadrupole results from the tilting of horizontal vorticity from both ambient vertical shear and the horizontally sheared plume.

By around 0.8-0.9 hr, deep, moist convection is initiated in most experiments. In the case of no shear, an upright tower of convection forms, reaching a maximum height of 16.4 km (Table 1). Soon after, a

centralized downdraft and axisymmetric, surface cold pool form. Moderately vigorous downdrafts occur in this storm, reaching 11 m s^{-1}, which is consistent with the dry air in the initial sounding (Figure 1). After the cold pool forms, secondary updrafts arise symmetrically on the cold pool edges. Hereafter defining a convective event to encapsulate any period over which the updraft exceeds 2 m s^{-1} at mid-levels (5.5 km), then the lifetime of the unsheared convective events is 1.8 hr.

Vertical shear takes away the axisymmetric structure of convection. The tower leans over toward the north with the shear and produces a preferential downdraft down-shear of the storm. The storm updraft takes on a U-shaped pattern and even splits into two cells in the strongest vertical shear case. The western and eastern cells rotate anticyclonically and cyclonically, respectively, due to the tilting of horizontal vorticity. As seen in Table 1, vertical shear decreases the lifetime of the storms. Examination of the cold pool shows an increasingly vigorous cold pool with increasing vertical shear. These results, along with the increasing downdraft speed with increasing shear, come about from the dry air aloft. Interestingly, the highest cloud tops obtained occur for storms in the highest vertical shears, where v_z = 20 m s^{-1} (15 km)$^{-1}$ yields a substantial maximum cloud top of 17.4 km. Dynamic pressure perturbation analysis is being carried out to determine if the additional lift caused by a rotating updraft contributed to this result.

Figure 3. Derivative components (shaded) in the rotated coordinate system of the tilting term (2) for v_x = -6 x 10^{-4} s^{-1} and v_z = 0. The total tilting term (x 10^{-6} s^{-2}) is superimposed (solid contour is 1 x 10^{-6} s^{-2}; broken contour is -1 x 10^{-6} s^{-2}).

	τ_{conv}	h_{conv}	w_{max}	w_{min}
Exp. 0,0	1.8	16.4	39.7	-11.5
Exp. 0,5	1.0	16.4	39.4	-14.5
Exp. 0,10	0.9	16.4	36.8	-14.8
Exp. 0,20	0.9	17.4	35.4	-13.4
Exp. 2,0	0.9	15.9	32.0	-9.7
Exp. 2,5	1.0	15.9	35.1	-10.7
Exp. 2,10	0.9	17.9	34.8	-12.8
Exp. 2,20	1.1	16.4	34.6	-12.1
Exp. 4,0	1.0	13.4	25.8	-8.9
Exp. 4,5	1.0	14.4	31.0	-8.6
Exp. 4,10	1.0	13.9	30.7	-10.1
Exp. 4,20	0.9	15.4	28.2	-9.7
Exp. 6,0	0.2	8.4	15.4	-5.6
Exp. 6,5	0.2	9.4	17.4	-5.6
Exp. 6,10	0.4	9.9	16.9	-5.7
Exp. 6,20	0.5	9.4	19.9	-6.8

Table 1: Convective lifetimes, τ_{conv} (hr), maximum height of convection, h_{conv} (km), maximum updraft speed, w_{max} (m s^{-1}), and minimum updraft speed, w_{min} (m s^{-1}), for all experiments. Exp. α,β means v_x = -α x 10^{-4} s^{-1} and v_z = β m s^{-1} (15 km)$^{-1}$.

Horizontal shear also plays a significant role on the evolution of convective storms. Figure 4 presents midlevel vertical velocity fields throughout the lifecycle of a horizontally sheared storm. The general behavior for horizontally sheared storms includes filamentary elongation along the plume ellipse, subsequent splitting into two oppositely moving and elongating storm cells, followed by eventual decay. The strength of the shear controls how rapidl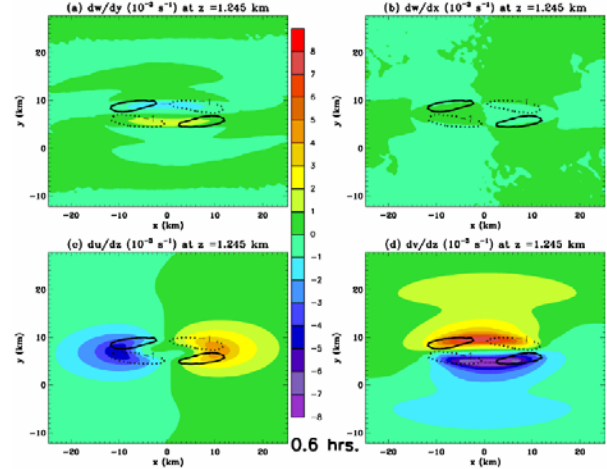y this process occurs. As Table 1 shows, horizontal shear strongly regulates the strength of a storm. Simply increasing the horizontal shear decreases the storm lifetime, the maximum heights of the storm, and the strength of vertical motions. The filamentation of storms increases the area of updraft exposed to midlevel dry air, which increases entrainment, and therefore, decreases convective instability.

Unlike in the case of the filamentation of a passive tracer or vorticity (Rozoff et al. 2006), horizontal shear leads to storm splitting. As the storm matures, precipitation begins falling through the center of the storm. As a cold pool forms and deforms in the shear, the atmosphere is rapidly stabilized near the center of convection. Only the updrafts at the ends of the filamentary structure are left to ingest the relatively warm and moist environmental air necessary for storm sustenance.

As in a real hurricane, the bulk of the experiments contain a combination of shears. The results of these experiments contain a hybrid of properties seen in previous results. As indicated in Table 1, for a given nonzero, horizontal shear, vertical shear can actually increase the maximum cloud height, vertical motions, and even the lifetime in some cases. Sample midlevel vertical motion fields of the experiment containing v_x = -4 x 10^{-4} s^{-1} and v_z = 10 m s^{-1} (15 km)$^{-1}$ are provided in Figure 5. Interestingly, the southern storm dominates in the beginning of this convective event, while a second storm cell emerges on the northern edge of the cold pool later on in the evolution. Further analysis of the storm dynamics is underway.

4. EFFECTS ON THE MEAN FLOW

Even though it is typically an asymmetric process, most convection will have some influence on the mean flow of the hurricane. While we are not simulating a full hurricane, we can gather some qualitative information on the effects our convective elements may have on the
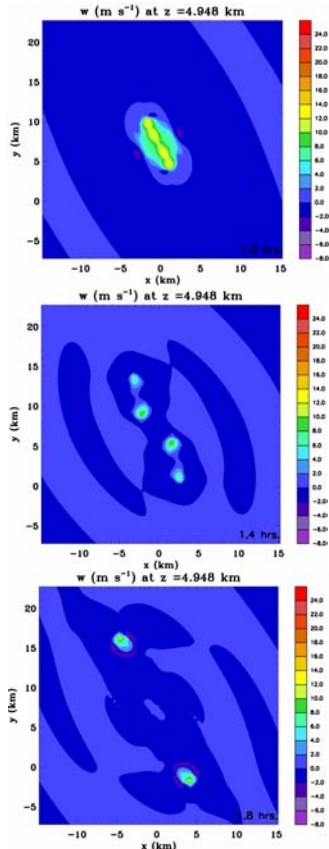
Figure 4. Vertical velocity (m s^{-1}) at z = 4.95 km at 1, 1.4, and 1.8 hr for the experiment with v_x = -4 x 10^{-4} s^{-1} and v_z = 0.

Figure 5. Vertical velocity (m s^{-1}) at z = 4.95 km at 1, 1.4, and 1.8 hr for the experiment with v_x = -4 x 10^{-4} s^{-1} and v_z = 10 m s^{-1} (15 km)$^{-1}$.

hurricane by looking at the along-wind mean flow changes.

Examination of the mean potential vorticity (PV) changes (Figure 6) after the end of the active convection period shows some interesting results. First, horizontal shearing alone tends to have a symmetrizing and weakening effect on the mean PV changes. Vertical shear alone, however, leaves an asymmetrical mean PV change pattern, due to the strong tilting of the environmental horizontal vorticity into the vertical where the isentropic gradients are stronger. The combination of horizontal and vertical shears tends to force a mean PV change that is generally asymmetric, but tilted in height. The exact reasons for the emergence of this pattern are still under investigation, but are nonetheless intriguing.

Other mean fields show expected results. The mean potential temperature change shows a slight warming near the mid-layers and a cold pool near the surface, indicating the immediate stabilization of this region of the mean vortex to additional convection. However, given the thermodynamic sensitivity of convection in this particular sounding (to be discussed shortly), later changes such as the advection of the shallow cold pool away from this area may leave a region that is even more favorable for convection than before, thanks to the increased moisture in the atmosphere.
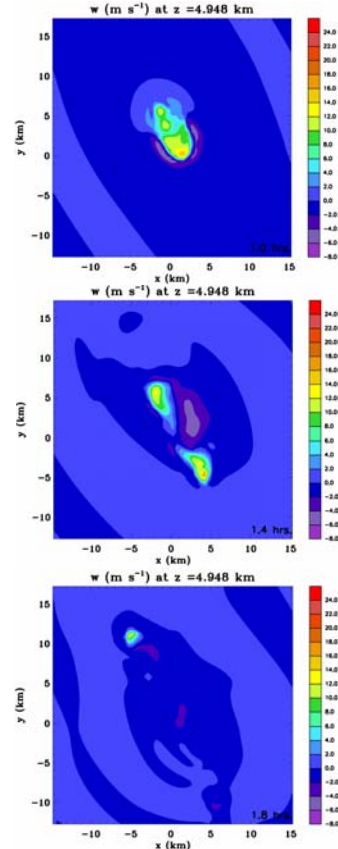
Kinematic fields show a slight spin-up of vorticity in the mean, particularly at the lowest model layers. Additionally, there seems to be some evidence of a cyclonic/anticyclonic vortex asymmetry favoring cyclonic vorticity. Understanding exactly how these kinematic fields are changed by these basic convective elements is a strong step toward understanding changes to the kinematics of the hurricane vortex outside its core region.

5. THERMODYNAMIC SENSITIVITIES

The composite sounding used to initialize the previous experiments contains considerable dry air aloft, along with modest low-level parcel buoyancy. Given the thermodynamic variability outside the inner-core of a hurricane, the background temperature and moisture profiles of the previous experiments should not be expected to always hold outside an eye wall. To this end, two types of sensitivity experiments are carried out to uncover sensitivities of convection to background moisture and convective stability.

The first series of experiments increases the lower level instability in the 900 to 700 hPa layer such that the temperature at any given level in that layer does not cool more than 1 K. This minute change in lapse rate results in an increase of 53 J kg^{-1} of CAPE. Four
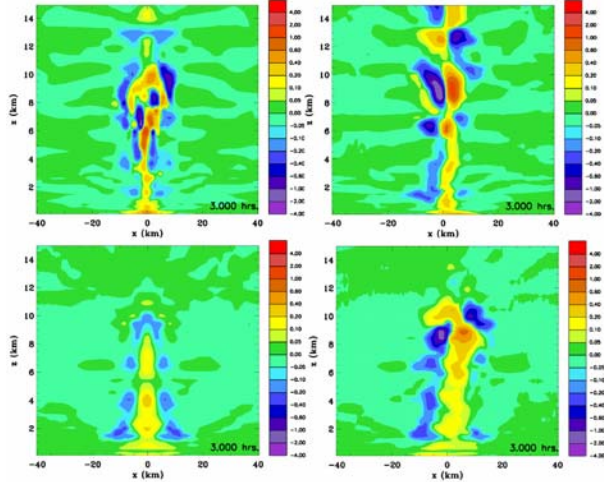
Figure 6. Meridionally-averaged mean potential vorticity (PV) difference from the initial PV (PVU) at 3 hr, where the top row is for $v_x = 0 \times 10^{-4}$ s^{-1}, the bottom row $v_x = -4 \times 10^{-4}$ s^{-1}, the left-column $v_z = 0$ and the right-column $v_z = 10$ m s^{-1} (15 km)$^{-1}$.

experiments are conducted covering all combinations of the highest magnitudes of shear and no shear. The results of the unstable experiments are summarized in Table 2. Unlike before, experiments with $v_x = -6 \times 10^{-4}$ s^{-1} now produce clouds with appreciable vertical depth (> 15 km) and much longer lifetimes. Likewise, the longevity and strength of the other storms increase too. Hence, a slight increase in low-level instability can make remarkable differences in the results obtained in the control experiments.

	τ_{conv}	h_{conv}	w_{max}	w_{min}
Exp. 0,0	2.1	18.4	42.1	-17.1
Exp. 0,20	1.1	18.4	41.2	-19.3
Exp. 6,0	1.0	15.4	30.6	-7.7
Exp. 6,20	1.5	15.9	30.3	-12.3

Table 2: Convective lifetimes, τ_{conv} (hr), maximum height of convection, h_{conv} (km), maximum updraft speed, w_{max} (m s^{-1}), and minimum updraft speed, w_{min} (m s^{-1}), for the unstable experiments. Exp. α,β means $v_x = -\alpha \times 10^{-4}$ s^{-1} and $v_z = \beta$ m s^{-1} (15 km)$^{-1}$.

To investigate the role of the cold pool and dry-air entrainment on storms, a second set of sensitivity experiments involves moistening the original composite sounding (figure not shown). Once again, the results are quite different from the control set of experiments. A weaker cold pool results from the storms, which is beneficial in some cases and detrimental in others. As in the unstable experiments, some of the most vigorous convection is the strongly sheared convection. In these cases, dry air entrainment is decreased and the cold pool intensity is not as overwhelming. In the case of unsheared convection, the weaker cold pool precludes the development of secondary convection that was characteristic of experiments with drier air aloft.

	τ_{conv}	h_{conv}	w_{max}	w_{min}
Exp. 0,0	0.5	18.9	45.9	-20.0
Exp. 0,20	1.3	18.4	37.2	-13.8
Exp. 6,0	0.8	16.4	30.0	-10.8
Exp. 6,20	1.1	15.9	31.4	-8.2

Table 3: Convective lifetimes, τ_{conv} (hr), maximum height of convection, h_{conv} (km), maximum updraft speed, w_{max} (m s^{-1}), and minimum updraft speed, w_{min} (m s^{-1}), for the moist experiments. Exp. α,β means $v_x = -\alpha \times 10^{-4}$ s^{-1} and $v_z = \beta$ m s^{-1} (15 km)$^{-1}$.

6. ACKNOWLEDGMENTS

7. REFERENCES

Cotton, W. R., and Coauthors, 2003: RAMS 2001: current status and future directions. *Meteor. Atmos. Phys.*, **82**, 5-29.

Klemp, J. B., 1987: Dynamics of tornadic supercells. *Ann. Rev. Fluid Mech.*, **19**, 369-402.

Möller, J. D., and M. T. Montgomery, 2000: Tropical cyclone evolution via potential vorticity anomalies in a three-dimensional balance model. *J. Atmos. Sci.*, **57**, 3366-3387.

Möller, J. D., and L. J. Shapiro, 2005: Influences of asymmetric heating on hurricane evolution in the MM5. *J. Atmos. Sci.*, **62**, 3974-3992.

Montgomery, M. T., and R. J. Kallenbach, 1997: A theory for vortex Rossby-waves and its application to spiral bands and intensity changes in hurricanes. *Q. J. R. Meteorol. Soc.*, **123**, 435-465.

Rozoff, C. M., W. H. Schubert, B. D. McNoldy, and J. P. Kossin, 2006: Rapid filamentation zones in intense tropical cyclones. *J. Atmos. Sci.*, **63**, 325-340.

Weisman, M. L., and R. Rotunno, 2004: "A theory for strong long-lived squall lines" revisited. *J. Atmos. Sci.*, **61**, 361-382.

Willoughby, H. E., J. A. Clos, and M. G. Shoreibah, 1982: Concentric eye walls, secondary wind maxima, and the evolution of the hurricane vortex. *J. Atmos. Sci.*, **39**, 395-411.